Assessment of rock wool as support material for on-site sanitation: hydrodynamic and mechanical characterization

Adrien Wanko, Julien Laurent, Paul Bois, Robert Mosé, Christiane Wagner-Kocher, Nadia Bahlouli, Serge Tiffay, Bouke Braun, Pieter-Willem Provo Kluit

Assessment of rock wool as support material for on-site sanitation: hydrodynamic and mechanical characterization

Adrien Wanko[a*], Julien Laurent[a], Paul Bois[a], Robert Mosé[a], Christiane Wagner-Kocher[b], Nadia Bahlouli[a], Serge Tiffay[c], Bouke Braun[d] and Pieter-Willem Provo kluit[d]

[a]Icube, UMR 7357, ENGEES, CNRS, Université de Strasbourg, 2 rue Boussingault, 67000 Strasbourg, France; [b]LPMT, EA 4365, Université de Haute-Alsace, 11 rue Alfred Werner, 68093 Mulhouse Cedex, France; [c]Rockwool France SAS, 111 rue du Château des Rentiers, 75013 Paris, France; [d]Rockwool B. V., Industrieweg 15, 6045 JG Roermond, The Netherlands

This study proposes mechanical and hydrodynamic characterization of rock wool used as support material in compact filter. A double-pronged approach, based on experimental simulation of various physical states of this material was done. First of all a scanning electron microscopy observation allows to highlight the fibrous network structure, the fibres sizing distribution and the atomic absorption spectrum. The material was essentially lacunar with 97 $\pm$ 2% of void space. Static compression tests on variably saturated rock wool samples provide the fact that the strain/stress behaviours depend on both the sample conditioning and the saturation level. Results showed that water exerts plastifying effect on mechanical behaviour of rock wool. The load–displacement curves and drainage evolution under different water saturation levels allowed exhibiting hydraulic retention capacities under stress. Finally, several tracer experiments on rock wool column considering continuous and batch feeding flow regime allowed: (i) to determine the flow model for each test case and the implications for water dynamic in rock wool medium, (ii) to assess the rock wool double porosity and discuss its advantages for wastewater treatment, (iii) to analyse the benefits effect for water treatment when the high level of rock wool hydric retention was associated with the plug-flow effect, and (iv) to discuss the practical contributions for compact filter conception and management.

Keywords: compact filter; hydrodynamic; mechanical; on-site sanitation; rock wool

1. Introduction

On-site sanitation is both a technologically competitive and economically sustainable alternative to collective sanitation,[1] with water reuse possibilities.[2] Its principle is based on collection, transport, treatment and discharge of wastewater from buildings not connected to a public wastewater network. These systems are typically installed to treat grey and toilet wastewaters in areas without sewer and centralized treatment systems,[3] including very constrained site.[4] On-site sanitation installation is based on a two-step process: (1) primary treatment (septic tanks, primary filters and skimming tank) to screen solids and large wastes and (2) secondary treatment to biologically treat domestic wastewaters.

On-site sanitation was classified into three types by Lakel [5]:

- Micro-stations integrate both primary and secondary treatment; secondary treatment is achieved through action of settled or free biological population, with or without forced aeration. Treated effluent is then clarified and sludge is submitted to recirculation.
- Reed bed filters conjugate filter materials (sand, gravel), treating biomass and plants whose rhizosphere favours biomass formation, water infiltration and oxygen transfer.
- Compact filters implement fine material (sand, zeolite, rock wool, biologically sourced fibres) to treat aerobically through non-saturated filtration.

Many different techniques are marketed under the name of compact filters for the purpose of on-site sanitation. The difference lays in the nature of the filtration/colonization medium. Acknowledged media are sand, zeolite, coco fibres, rock wool, polonite, expanded schist, as well as other materials issued from mineral or organic wastes.[6] By importance, the commonly used filter materials are categorized as natural materials, industrial by-products and man-made products.[7]

The choice of filter materials is very important: it will influence filter dimensions, treatment efficiency and adaptation to load variation as well as technical implementation, maintenance and expenditures (investments, operation and maintenance). However, there is a lack of knowledge on

*Corresponding author. E mail: wanko@unistra.fr

filters filled with coco fibres and rock wool.[6] One may ask if the small number of rock wool-based filters is due to the lack of scientific knowledge on this medium. Indeed, many scientific studies on wastewater treatment potential by compact filters were conducted.[8–17] In these studies, very good treatment efficiencies were obtained on the basis of simple design considerations and short-time experiments. Yet, almost no thorough study on filling media's mechanical behaviour was conducted. While mechanical study could help in understanding long-term behaviour of granular media inside compact filters.

According to Bouchet [18] the market for on-site sanitation in France is under tension because individual financial efforts needed to obtain improved sanitation are expensive. Kaminsky and Javernick [11] analysed the high failure rate that affects on-site sanitation infrastructures. They concluded that technological knowledge on these systems must be supplemented.

Table 1 summarizes main design criteria for compact filters based on the rock wool filling medium. These basic criteria are essentially empirical and based on manufacturers' experience, which also explains their variability. Figure 1 illustrates the general structure of the compact filter incorporated in the on-site sanitation system. The thicknesses of the filtration layers, the size of rock wool cubes and the aeration pipes have a significant impact on the compact filter's effectiveness. If inappropriate design and operation are used, the treatment performance of these systems is not satisfactory in the removal of pathogens and organic matters.[3]

This study proposes mechanical and hydrodynamic characterization of rock wool for the purpose of biological filtration in on-site sanitation systems. This double-pronged approach, based on experimental simulation of various physical states of the rock wool, is intended to bring thorough knowledge of this medium when it is used in compact filters. What are the mechanical and hydrodynamic behaviours of rock wool that impact the design and the processing performances of compact filters in on-site sanitation? The classical rock wool material that is used for insulation is hydrophobic, whereas the tested material has been made of hydrophilic material.

2. Material and methods

2.1. *Scanning electron microscopy observations*

Scanning electron microscopy (SEM) observations were made with JSM 6700F NT based on a new cold-filed emission gun electron source and employing state-of-the-art computer control and imaging. A conical FE gun and semi-inlens objective generated high-resolution images. These observations enabled (1) observation of the fibrous network structure; (2) determination of fibre orientation distribution and size at a microscopic level, with ImageJ – Orientation J software and (3) determination of atomic absorption spectrum, with Desktop Spectrum Analyzer software (NIST DTSA-II).

2.2. *Stress–strain characteristic in compression*

2.2.1. *Test specimens and testing equipment*

2.2.1.1. Material and specimens Rock wool belongs to the foam family. In order to identify the mechanical behaviour of the studied foam, typical stress–strain curves

Table 1. Rock wool compact filters design parameters.

Pre-treatment	Sizing criteria			Filter materials renewal	Treatment efficiency
Septic tank	EH 1–10	V (m^3) 0.50–0.83	S (m^2) 0.26–0.43	4–10 years	TSS < 30 mg/L BOD < 35 mg/L

Note: BOD: biological oxygen demand, TSS: total suspended solid.

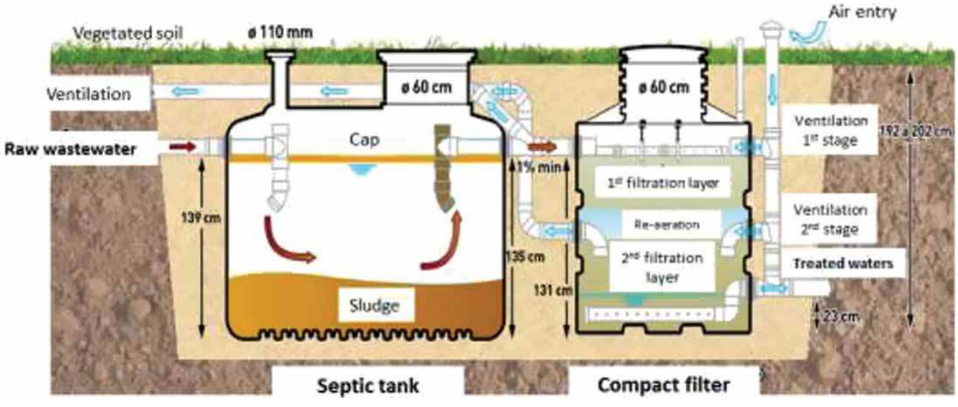

Figure 1. Diagram of onsite sanitation incorporating a compact filter (Source: COMPACT'O ®).

Figure 2. Directions of compressive load working: (left) in production line direction, (right) perpendicular of the product surface.

Figure 3. Examples of 80 mm (left) and packed 20 mm (right) rock wool cubes.

were obtained from quasi-static compression tests. It is known that the majority of the fibres are oriented in the horizontal direction in the Rockwool mineral wool products. This fibre orientation leads to anisotropy in the mechanical behaviour. Therefore, cuboid compression specimens were cut in the transverse (production line direction) and longitudinal directions (perpendicular to the product surface). The direction of the compressive load working with regard to the fibres orientation in the specimen is shown in Figure 2. Due to the different sizes of cubes used in the filter, and due to the particular geometry of the foam, three different specimen sizes of the material were tested: 80 mm side cubes, 10 mm side cubes packed in cubic nets of 80 mm side and 20 mm side cubes packed in cubic nets of 80 mm side (Figure 3). Cubes are packed to reproduce as closely as possible actual use conditions in compact filters. Three specimens for each condition were performed. This number of tests was enough to validate the reproducibility of the test.

2.2.1.2. Quasi-static compression tests Quasi-static compression tests were conducted at room temperature and at relative humidity. A servo-hydraulic mechanical testing machine (Instron 8800) was used in displacement control at a rate of 8 mm/min corresponding to the standard velocity (thickness/10). Data acquisition was performed with integrated data processing program WaveMatrix software. The compressive loading platens were lubricated with PTFE spray in order to minimize friction between the specimen and platens. The cuboid specimens were compressed to large nominal strain up to 90%.

Three different states of water saturation were considered during the compression tests. The dry state was the initial samples packaging, average mass of dry samples was 50 g $\pm$ 3 g. Then, samples were completely saturated, thanks to slowly rising water imbibition during 24 h. Samples under residual water saturation were obtained after free and slow drainage during 24 h. For the three different

states of water saturation, force displacement curve and water flow were recorded.

2.3. Hydrodynamic properties assessment

2.3.1. Density, permeability and water retention

Actual bulk and solid densities were determined with pycnometers. Saturated hydraulic conductivity (Ks) was determined with a constant load permeameter, whose principle is based on Darcy's Law. This hydrodynamic parameter gives indeed information on water and chemical transport within the porous media. Hydrodynamical behaviour of a variably saturated material is well represented by the hydraulic retention curve that depends on both texture and material structure, and exhibits material capacity to retain water. In order to determine hydraulic retention in small tension range ($h < 500$ cm; pF < 2.7), the kaolin/sand box method was used.[19] This method allows simple, reliable and cheap measurements on raw 250 cm^3 material samples.

2.3.2. Tracer tests and residence time distribution analysis

In ecological engineering field, it is widely acknowledged that tracer experiments are of utmost interest for transport properties assessment and to investigate the impact of management operations on treatment facilities.[20–23] A well-conducted experiment brings information on flow regime, dispersion regime and residence time distribution (RTD). RTD and mixing dynamics have been studied in filtration columns that mimic compact filter filled with rock wool, in both continuous and discontinuous (batch mode) hydraulic modes. Cylindrical columns (Figure 4) of 200 mm diameter, 500 mm height and made out of Plexiglas have been built for this purpose. A perforated Plexiglas plate (holes diameter: 3 mm) placed at the bottom enables filtration. From bottom to top, the filter material filling the column (Figure 4) was made of 5 cm layer of fine gravel (4–8 mm size), 15 cm layer of small rock wool cubes (10 mm edge) and 15 cm layer of coarse rock wool cubes (20 mm edge). Water was fed from the top of the column by a peristaltic pump. Sodium chloride (NaCl) was used as a tracer; a known amount of salt (50 ml at 75 g/l) was injected instantaneously on the top of the column. Outlet concentration was monitored every 5 s with a conductivity probe (TetraCon 325 probe) linked to a multi-parameter analyser (MultiLine P4). Conductivity probe calibration led to a linear relationship between concentration C (g/L) and electrical conductivity σ (µS/cm):

$$C = (0.538 \pm 0.009) \cdot \sigma .$$

Desorption tests were performed to ensure that no ions were released by rock wool in aqueous solution, which could interfere in conductivity measurements. Fifty grams of dry rock wool was steadily stirred in 1 L of water during 3 h. Solution electrical conductivity was measured every 30 min and remained constant throughout the test. No interfering ion release was then likely to occur and tamper with conductivity measurements during tracer experiments.

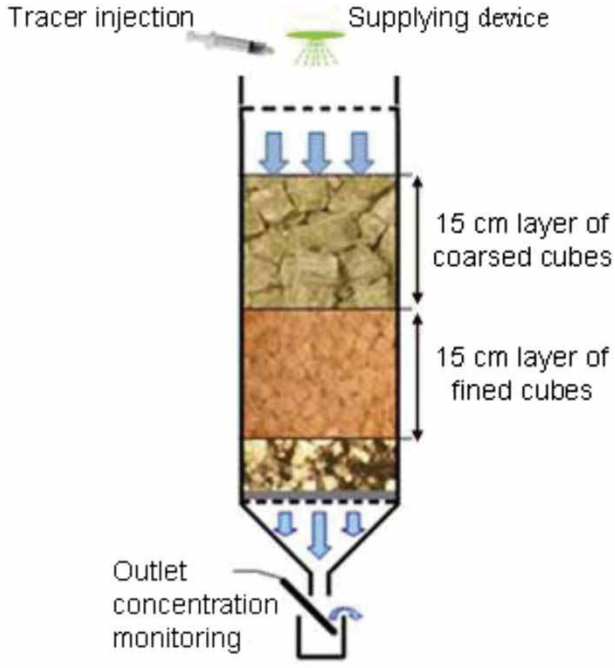

Figure 4. Experimental device for RTD calculation using tracer tests.

Table 2. Synthesis of flow rate for tracer experiments.

Feeding mode	Flow rate (ml/min)
Continuous (without ponding)	89; 190; 307; 393
Batch feeding (12 batches per day)	650 mL/batch every 2 h

The hydrodynamic behaviour of the filtration column filled with rock wool was analysed for four different continuous flow rates and one batch feeding, thus getting close to feeding conditions observed in on-site sanitation. Table 2 summarizes the different hydraulic conditions for realized tracer experiments.

Outlet concentration $C(t)$ was plotted as a function of elapsed time since tracer injection t. The residence time distribution function $E(t)$ is given by

$$E(t) = \frac{Q(t) \cdot C(t)}{M},$$

where $Q(t)$ is the flow rate and M is the total mass of tracer injected in the column. Time moment analysis [24] was applied to characterize the shapes of experimental breakthrough curves (BTC) in terms of mean breakthrough time and degree of spreading. Other parameters from RTD analysis could enhance the understanding of the hydrodynamic

behaviour of the system [25]: maximum flow velocity (V_{max}), mean flow velocity (V_{mean}) and nominal residence time (t_N). Finally, considering the different flow concepts [26] to model the RTD data and using other data treatment approaches,[26–28] the parameters below are calculated:

- The Peclet number (a dimensionless number that represents the advective and dispersive contributions to solute transport):

$$Pe = \frac{UL}{D},$$

where U is the axial mean velocity (m/s), L is the column length and D is the dispersion coefficient (m^2/s).

- The number N of continuous stirred tank reactors from a tank-in-series model:

$$N = \frac{1}{\sigma_\theta^2},$$

where σ_θ^2 is the dimensionless RTD variance obtained by the ratio between the RTD first-order and second-order time moments.[24]

3. Results and discussion

3.1. MEB observations and physico-chemical properties

Rock wool displays an essentially lacunar structure where matter is structured as crossed fibres and scattered balls. Figure 5 presents magnified pictures of horizontally cut samples.

Fibre diameters range from 2 to 25 μm (cf. Figure 6(a) and 6(c)). Rock wool balls are visible on Figure 6(b) and 6(d); their sizes range from 100 to 200 μm. These balls are formed when fibre formation was not achieved during the manufacturing process.

Analyses of main directions in the material showed a prevailing horizontal direction (the production line direction, see Figure 2) on the microscopic scale. On a centimeter scale – the actual scale of use in compact filter – horizontal layers with anisotropic fibres repartition were observed. It can be assumed from these preliminary observations that an important void space was present in the material.

Atomic spectra of all analysed samples were similar, which indicates homogeneous matter composition. Atomic and mass composition of rock wool is indicated in Table 3.

Na, K and P chemical elements are present as well, although in much lesser quantity than magnesium (Mg). This essentially mineral composition will influence (i) interactions between material and wastewater content and (ii) ageing of the material.

3.2. Results of experimental mechanical tests

3.2.1. Load working direction dependence

Static compression tests for 80 mm side cubes were performed on parallel and perpendicular planes to compression direction, stress–strain curves were then plotted. The nature of the stress–strain curve divided into three regions was almost similar for all the cases. Thus, Figure 7 highlights typical rock wool behaviour phases for the specimen tested.[29] Within the first linear elastic region, stress is directly proportional to strain. As the value of stress increases, strain also increases simultaneously. The initial slope in the linear elastic region is Young's modulus of the rock wool. The second region is a plateau region where stress oscillates (increases and decreases) with strain for the longitudinal test. The third region is the densification region, where the slope of the stress–strain curve suddenly increases due to consolidation of the structure.

The densification strain is defined as the intersection point between the horizontal strain axis and the extension of the linear densification end-part of the curve. This method has already been used to determine organic foams compression characteristics.[30] In the longitudinal direction, two typical characteristics were identified from these curves: the cell collapse stress (0.08 MPa) and the locking strain or densification strain (0.7).

Behaviour during the elasticity phase differs between sample orientations, as shown on Figure 7: initial slope is steeper when the compression direction is parallel to the main material direction. A local buckling was observed for this configuration. From the compact filter point of view, stress will be assimilated to the whole structure weight with different water saturation levels.

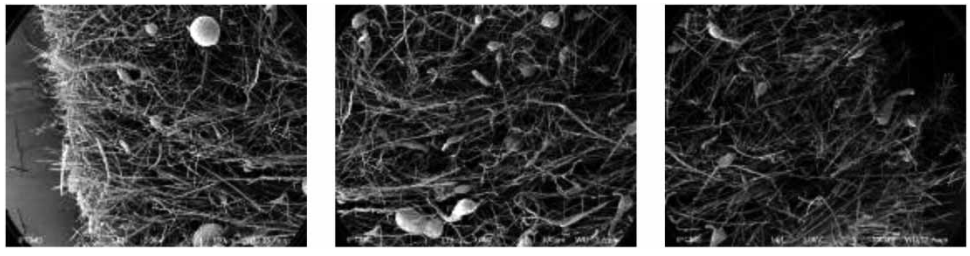

Figure 5. Observations of a three piece rock wool sample.

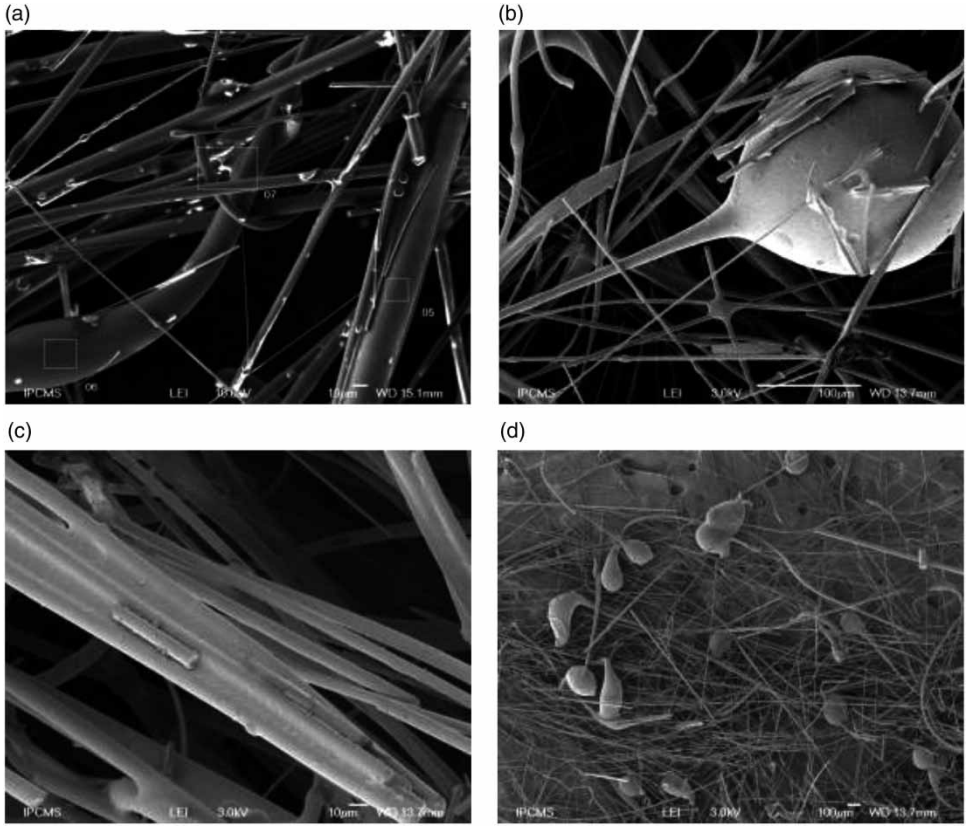

Figure 6. Solid matrix structure illustration (a) relative fibre sizes, (b) ball at the end of a fibre, (c) fibre binder and (d) ball scattering.

Table 3. Atomic and mass composition of rock wool main components.

Element	O	Si	Al	Ca	Fe	Mg
Atom (%)	60.55	14.27	7.15	6.94	4.63	4.32
Weight %	42.78	17.70	8.52	12.29	11.42	4.63

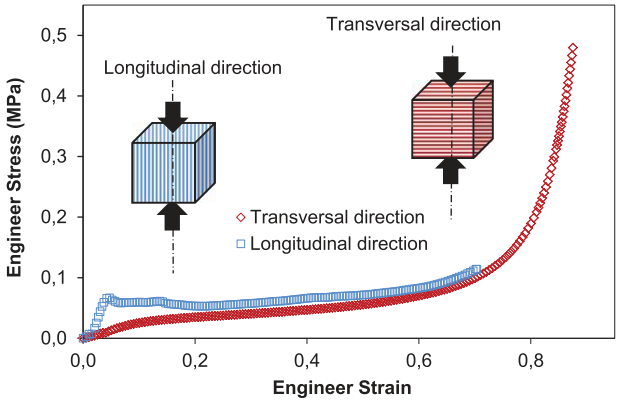

Figure 7. Mechanical stress tests on rock wool cube of 80 mm side: a study of the anisotropy.

3.2.2. *Influence of water saturation level*

Analysis of curves (cf. Figure 8) shows that dry materials were stiffer than variably saturated ones. Hence, the more saturated the material, the more deformed it gets. Plateau indicating plastic phase was longer for water containing samples. It can then be assumed that water exerts a plastifying effect on mechanical behaviour of rock wool.

3.2.3. *Hydromechanical behaviour of bagged rock wool*

Packed cubes compaction level increases with saturation level, conversely to what was observed with 80 mm side cubes. Wet packed cubes get more reluctantly crushed than dry ones, whatever the cube dimension considered (Figure 9). At equal displacement of the compression plateau, 20 mm side cubes were more easily compactable than 10 mm side cubes. This very important result evidences additional elements to justify the stacking order of rock wool cubes layers (Figure 4).

Tests performed on variably saturated samples allowed determining: (1) maximal displacement of the compression plateau before water flow (threshold displacement) and (2) drainage flow rate from rock wool under stress. Water retention capacity strongly influences hydraulic residence time through the material and thus contact time between fluid and solid matrix. Figure 10 shows threshold displacements and drainage flow dynamics of samples for different cube sizes and two water saturation levels.

Regardless of the water saturation level, the drainage flow rates were the same (1.51 ± 0.2 g/s) for 10 and 20

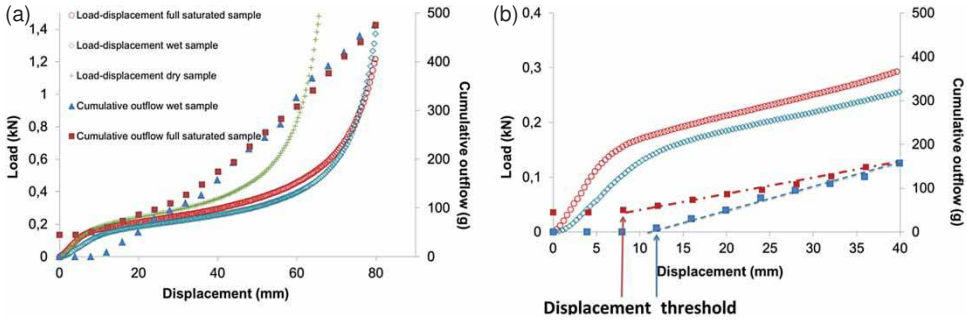

Figure 8. (a) Load–displacement curve on rock wool cube of 80 mm side: the water saturation impact and (b) magnification of (a): identification of the displacement threshold.

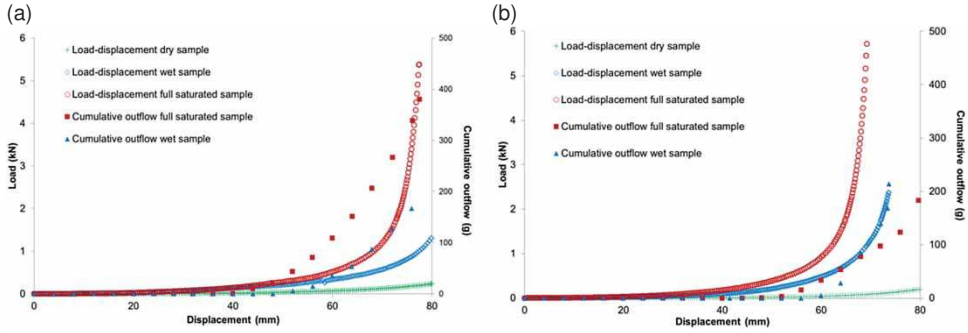

Figure 9. Cumulative outflow measurements under compression on bagged small rock wool cube of 20 mm side (left) and 10 mm side (right): the water saturation impact on the load–displacement curve.

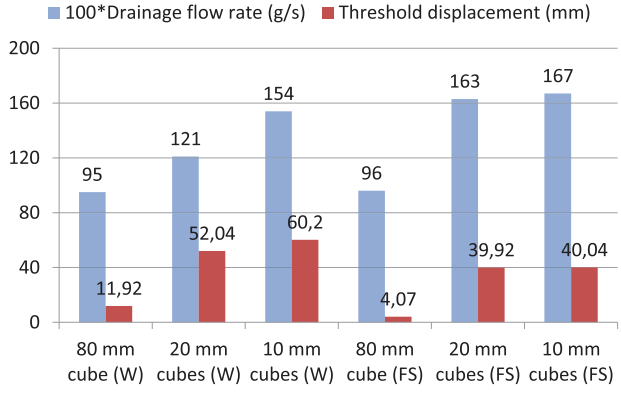

Figure 10. Threshold displacement and drainage flow rate for different rock wool configurations and saturation (FS: full-saturated sample; W: wet sample).

mm bagged samples. These flow rates were higher than those of 80 mm samples (Figure 10). Similar observations were made for the thresholds displacement. Moreover, the lower the saturation level, the higher the capillary pressures. Hence, the smaller thresholds were obtained for full-saturated samples. This would lead to the fact that if the filter water supply occurred while it was fully saturated; the hydraulic residence time would be shortened. A batch feeding would instead alternate wetting and drainage phases, increasing the hydraulic retention time due to higher thresholds displacement for unsaturated rock wool filter materials. The following section provides a more detailed understanding on the rock wool hydrodynamic behaviour in the filter.

3.3. *Hydrodynamic behaviour of rock wool*

3.3.1. *Density and porosity*

According to pycnometer tests, rock wool displayed a solid density of 2.7 ± 0.1 (12 measurements), an apparent wet density of 1.1 ± 0.3 (8 measurements), an apparent dry density of 0.08 ± 0.01 (8 measurements) and a total porosity of 97 ± 2% (8 measurements). These results confirm microscopic observations that showed an essentially lacunar material. Solid density allows assessing vertical stress distribution in a dry filter under gravity; this is the minimal stress. Maximal stress was obtained from apparent wet density. Matter dynamics and exchanges inside the compact filter are likely to be enhanced by material's high porosity.

3.3.2. *Rock wool hydric retention curve and permeability*

Following protocol described in Section2.3.1, relations between capillary pressure and water content are given by the hydric retention curve in Figure 11.

Two main conclusions can be drawn (i) rock wool-saturated water content was more than twice as high as those from the classical natural granular media such as sand, loam, clay and silt and (ii) a high variation range of

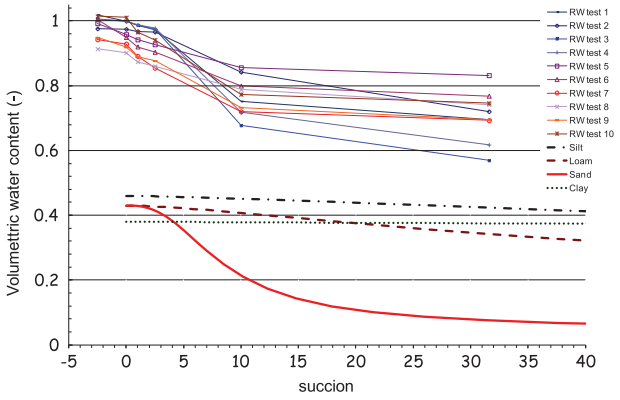

Figure 11. Characteristic curves of 10 rock wool samples are compared with known soils (Silt, Loam, Sand and Clay from Hydrus 2D/3D Manual).

water content was observed for both rock wool and sand. These properties will impact flows and reactive transfer dynamics inside the compact filter.

Rock wool-saturated permeability depends on cube sizes. Values range from 380 ± 120 cm/h (80 mm cubes) to 297 ± 43 cm/h (20 mm size cubes) and 860 ± 11 cm/h (10 mm side cubes). Saturated permeability depended largely on test tubes filling but still remained higher than the ones for sand filters (∼ 40 cm/h).

3.4. *Breakthrough curve and RTD analysis*

3.4.1. *Tracer curves in the continuous feeding mode*

Breakthrough curves (BTC) at the outlet of the column as a function of time are shown below.

Under a high flow rate regime, flow was well described by a plug-flow model: the highest peaks of concentration on a short time (Q1 and Q2). Whereas under low flow rate regime, dispersion seemed more important: the lowest peaks of concentration on a longer time (Q3 and Q4): it is a plug-flow model with high dispersion. Delay time decreased as the flow rate increased which is consistent. At Q2, Q3 and Q4 flowrates, the concentration peak and the BTC scattering increased with flow rate. This seems logical, given that flow rate decrease should favour inter-phases transfer within the filtration column. In turn this would favour more tracer dispersion, and a subsequent concentration peak decrease. However, this trend was not observed for the maximum flow rate (Q1). Does this fact have a physical meaning? Table 4 summarizes hydrodynamic features obtained from the tracer experiment.

A high tracer recovery was calculated for all the tracer experiments (0.95 ± 0.03). Theoretical, mean and maximal velocities decrease with increased flow rate as expected. As well as mean residence time, nominal time, delay time and statistical dispersion decreased in a power law as flow rate increased (Figure 12). Notably, t_{mean} and t_{50} curves were almost confounded; hence t_{50} was appropriated to simulate the experimental mean residence time. Conversely, the peaks concentration, the Peclet number, the dispersion coefficients and the number of tanks in series did not change monotonically (Table 4). A significant difference between low and high flow rates was observed. More data are necessary to draw a conclusion on the evolution of these parameters.

3.4.2. *Rock wool dual porosity concept*

BTC tail got longer as flow rate decreased. Indeed, slow dilution of the tracer for low flow rate was due to the increase in available mobile water content during water flow, hence mobile porosity. Whereas immobile water content defines dead volumes or immobile porosity. These two porosities were complementary and defined together

Table 4. Hydrodynamics parameters (computed from RTD).

Parameter	Q1	Q2	Q3	Q4
Tracer mass recovery (%)	0.960	0.950	0.985	0.911
Mass recovered at mean RTD (%)	0.520	0.480	0.590	0.510
Mean RTD (t_{mean}, s)	610.507	717.344	1346.878	2713.543
Nominal time ($t_{nom.}$, s)	1677.860	2199.115	3298.672	6597.345
Delay time ($t_{D.}$, s)	327.000	412.000	557.000	1067.000
Variance (s^2)	25399.468	30818.203	289008.677	1861131.911
Mean temperature (°C)	17.900	19.100	19.200	19.300
Peak concentration (g/l)	1.942	2.103	1.357	1.257
V_{max} (cm/s)	0.107	0.085	0.063	0.033
V_{mean} (cm/s)	0.057	0.049	0.026	0.013
$V_{theoretical}$ (cm/s)	0.021	0.016	0.011	0.005
Effective or mobile porosity	0.364	0.326	0.408	0.411
Immobile porosity	0.606	0.644	0.562	0.559
Peclet's number	32.915	37.005	15.743	10.834
Dispersion coefficient (m^2/s)	0.030	0.027	0.064	0.092
Mixing efficiency	0.600	0.507	0.727	0.736
N	16	19	7	5

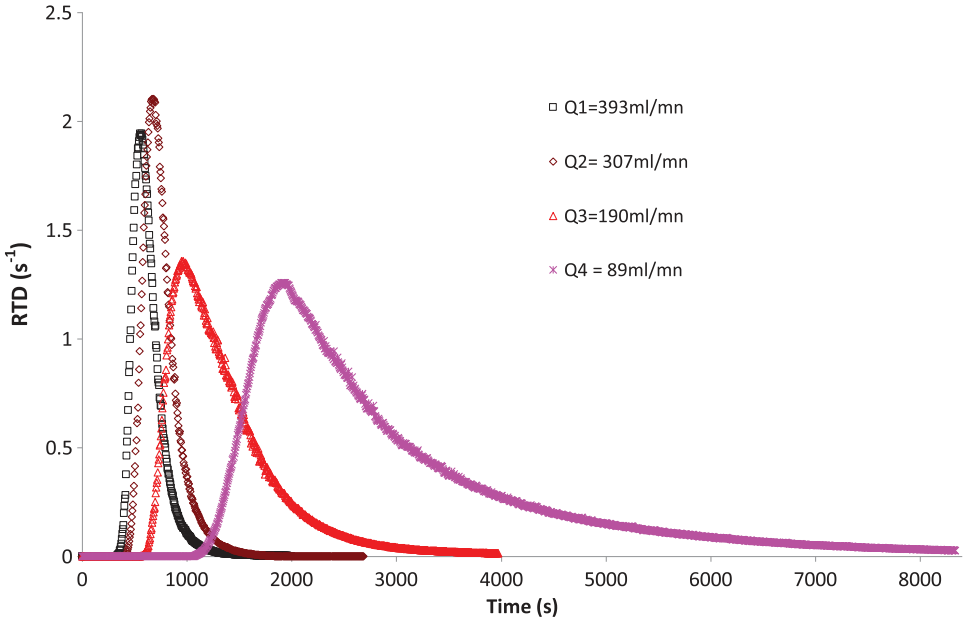

Figure 12. RTD from rock wool column at different flow rates.

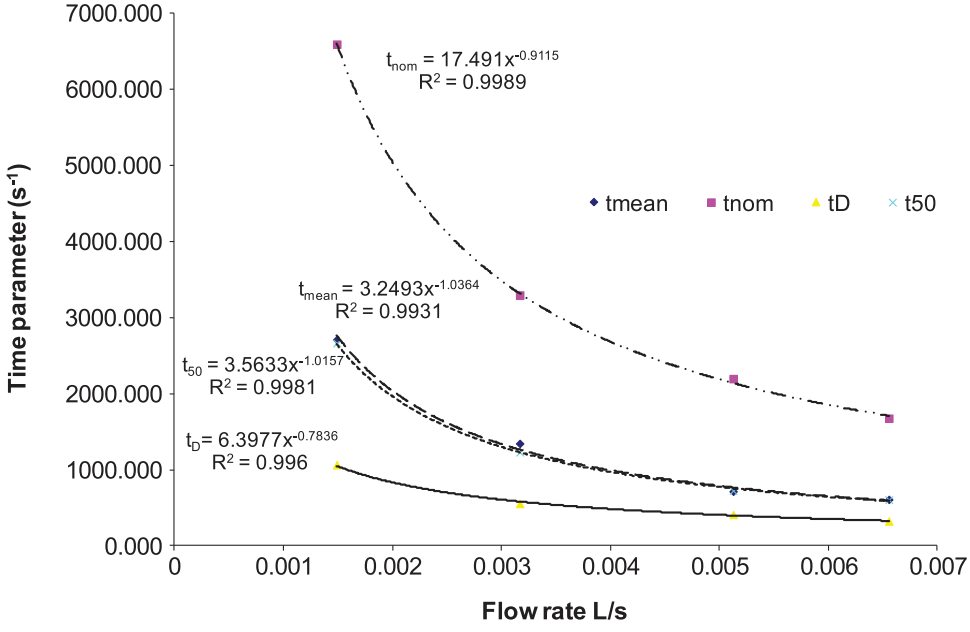

Figure 13. Model for time parameters variation.

the total porosity (0.97 ± 0.02, see Section 3.3.1). Fast water flow occurred in macroporosity, while the slow water flow occurred in microporosity, although transfers between these two-phases occur [31]: thus the double or the dual porosity is highlighted. In this paper, we define the mixing efficiency as the ratio of mobile to immobile porosity. The higher it is, the better should be the mixing in the mobile phase. Conversely, as immobile porosity decreases, transfers between phases will decrease. Table 4 and Figure 13 show that low flow rates (high mobile porosity) should favour exchanges in the mobile phase. But the transfer capacities were reduced due to low immobile porosity, so balance needs to be found. Double porosity model developed here was then significant in the batch feeding mode. (Figure 14)

3.4.3. Tracer responses in the batch feeding mode

The batch feeding mode was closer to on-site sanitation compact filter operation conditions. Due to pollutant degradation scale-time, the greatest part of pollution mitigation will actually occur during the resting phase: treatment is located in immobile porosity.[32,33] Hence the filter retention capacities should foster the contact time between

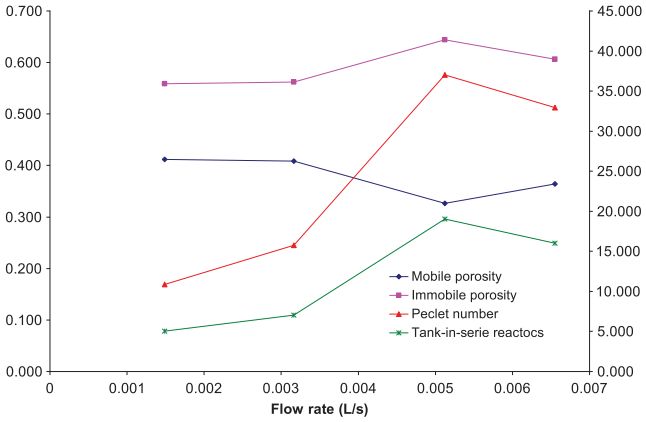

Figure 14. Mobile and immobile porosity (left axis), Peclet number and N variations (right axis).

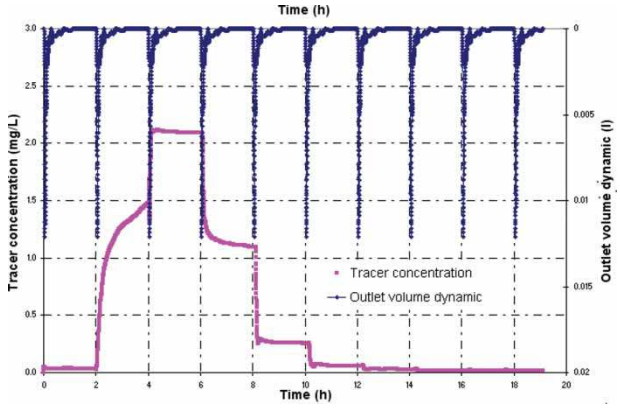

Figure 15. Outlet volume dynamic and tracer concentration during the tracer test.

liquid-phase pollution and the biofilm. A significant mobile porosity will provide ample oxygen renewal during the resting phase. This can be seen as a consequence of the strong water content gradient observed on rock wool (Figure 11).

As the hydraulic regime was no longer permanent, the theory of moments applied to RTD analysis should not be valid anymore. Cross-analysis curves of tracer concentration and outflow rate, as well as cumulated outlet tracer mass and cumulated volume can nevertheless be shown (cf. below Figures 15 and 16).

No tracer was detected at the outlet immediately after the first feeding event. The 0.65 L drained immediately after a new feeding (Figures 15 and 16) was the residual volume inside the column. This retention capacity and the plug-flow effect induced a tracer residence time much longer. Figure 15 shows that 50% of the tracer was recovered during the third batch, e.g. residence time of 6 h for 50% recovered mass. Considering t_{50} evolution curve with flow rate as established in the permanent regime (Figure 13), a 12 mL/min flow rate (very low) in steady-state conditions would be needed to obtain a similar residence.

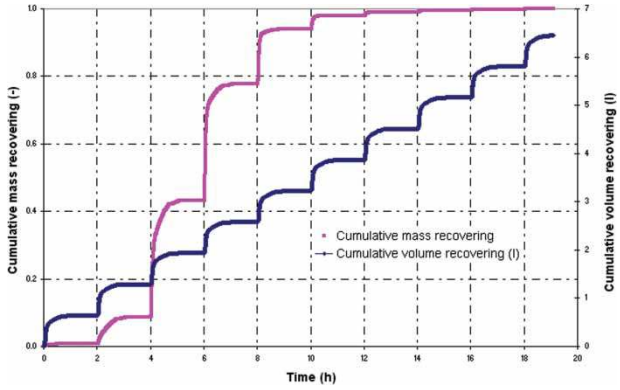

Figure 16. Cumulative volume and mass recovering during the tracer test.

3.4.4. *Practical contributions for design and expected pollutant removal rate*

The present work significantly contributes to the conception and management of compact filter with synthetic media in the framework of one-site sanitation. Indeed results from the compression test showed that coarse rock wool cubes were more easily compactable than the fine ones. If the filter was designed with several layers of different sizes of rock wool cubes, it is recommended to arrange them in decreasing size order, from top to bottom. Additionally it appeared that the rock wool-saturated water content and its dynamic range were substantially higher than those from classical granular media such as sand, loam, clay and silt. These hydrodynamic properties will favourably impact the reactive transfer and thus pollutant removal in compact filter.

Furthermore, using the tracer study results, the expected soluble pollutant (e.g, nitrogen) removal through the compact filter is estimated, thanks to the following mathematical model [21,23,28,34]:

$$\mathrm{RR}(\%) = \left(1 - \frac{C_{\mathrm{out}}}{C_{\mathrm{in}}}\right) \times 100 \quad \text{with} \quad \frac{C_{\mathrm{out}}}{C_{\mathrm{in}}} = \left(\frac{1}{1 + k.t_{\mathrm{mean}}/N}\right)^{N},$$

where $C_{\mathrm{out}}/C_{\mathrm{in}}$ is the pollutant fraction (of concentration) remaining at the outflow of a treatment, k is the volumetric reaction rate coefficient (h^{-1}) and RR the pollutant removal rate. The model illustrates the importance of hydraulic conditions for pollutant removal. Thus in this study, RR(%) = [15; 17; 30; 50], corresponding to the continuous flow rate Q (ml/min) = [393; 307; 190; 89] while RR = 71% for the batch feeding mode. Indeed, the batch feeding mode (closer to on-site sanitation compact filter operation conditions) increased the hydraulic retention time due to higher thresholds displacement for unsaturated rock wool filter materials. Eventually, the above mathematical model provides a means by which a simple tracer

pulse could be used to determine if changing hydraulic operations significantly change treatment function within an established compact filter.

4. Conclusion

Many different techniques are marketed under the name of compact filters for the purpose of on-site sanitation. Compact filters implement fine material such as sand, zeolite, rock wool, biologically sourced fibres, to treat aerobically through non-saturated filtration. This study proposes mechanical and hydrodynamic characterization of rock wool: a double-pronged approach, based on experimental simulation of various physical states of the rock wool. Below are the main results that are intended to bring thorough knowledge of this medium when used it in compact filters:

- Rock wool displays an essentially lacunar structure where matter was structured as crossed fibres and scattered balls. This result from MEB study has been confirmed by a porosity assessment of 97%: hence an important void space for water and matter exchanges.
- Static compression tests on dry rock wool sample highlighted three phases: linear elastic phase, stress plateau and densification phase; results showed that the plastic phase is longer for water containing samples.,
- Tests performed on variably saturated samples allowed determining: (1) maximum threshold displacement without flow and (2) drainage flow rate from rock wool under stress,
- Two main conclusions from water characterization curves: (i) rock wool-saturated water content was more than twice as high as those from the classical natural granular media such as sand, loam, clay and silt; (ii) a high variation range of water content was observed for both rock wool and sand. These properties should impact flows and reactive transfer dynamics inside the compact filter,
- The RTD analysis in the continuous water flow regime allowed to emphasis the dual porosity model in variably saturated rock wool column. The relative dynamics of mobile and immobile porosities were strongly related with the flow rate.
- Finally, the tracer experiment in the batch feeding mode (close to compact filter operation conditions) highlighted the fact that the high level of hydric retention and the plug-flow effect made the hydraulic residence time much longer.

Disclosure statement

No potential conflict of interest was reported by the authors.

References

[1] French Ministry of Ecology, Sustainable Development and the French Energy. Assainissement non collectif – Guide d'information sur les installations: Outil d'aide au choix; 2012. 47p. Available from: http://www.developpement-durable.gouv.fr/IMG/ANC_Guide-usagers_web_02-10-12_light.pdf

[2] Friedler E. Quality of individual domestic greywater streams and its implication for on-site treatment and reuse possibilities. Environ Technol. 2010;25(9):997–1008.

[3] Koottatep T, Eamrat R, Pussayanavin T, Polprasert C. Hydraulic evaluation and performance of on-site sanitation systems in Central Thailand. Environ Eng Res. 2014;19(3):269–274.

[4] Marseille JGSt, Anderson BC. Use of leaching chambers for on-site sewagetreatment. Environ Technol. 2010;23(9): 261–272.

[5] Lakel A. Installation d'assainissement autonome; conception, mise en oeuvre et entretien pour maison individuelle. Cstb – Guide Pratique. Sciences Appliquées Bâtiments Et Travaux Publics; 2012. 75 pages, 24×16 cm, 206 grammes.

[6] ASNC Network. "reseau rhone alpes des acteurs de l'anc" – graie. Retours d'experiences sur les filières d'assainissement non collectif: Document de travail evolutiv. Villeurbanne: 2011. 56p.

[7] Vohla C, Kõiv M, Bavor HJ, Chazarenc F, Mander U. Filter materials for phosphorus removal from wastewater in treatment wetlands – a review. Ecol Eng. 2011;37(1):70–89.

[8] Friedler E, Kovalio R, Ben-Zvi A. Comparative study of the microbial quality of greywater treated by three on-site treatment systems. Environ Technol. 2010;27(6):653–663.

[9] Prigent S, Belbeze G, Paing J, Andres Y, Voisin J, Chazarenc F. Biological characterization and treatment performances of a compact vertical flow constructed wetland with the use of expanded schist. Ecol Eng. 2013;52:12–18.

[10] Guyard C. Compact filters: reliable, simple and proven systems [Filtres compacts: Des solutions fiables, sobres, qui font leurs preuves]. Eau, l'Industrie, les Nuisances. 2013;358:61–68.

[11] Kaminsky J, Javernick-Will A. Causes for sustainable maintenance and operation of on-site sanitation systems. Construction Research Congress. May 21–23; West Lafayette, Indiana, United States; 2012. p. 2270–2279.

[12] Kasak K, Karabelnik K, Kõiv M, Jenssen, PD, Mander Ü. Phosphorus removal from greywater in an experimental hybrid compact filter system. 6th International Conference on Sustainable Water Resources Management, WRM 2011; Riverside, CA; United States; 23 May 2011 through 25 May 2011; Code 92380. WIT Trans Ecol Environ; 145: 649–657.

[13] Renman A, Hylander LD, Renman G. Transformation and removal of nitrogen in reactive bed filter materials designed for on-site wastewater treatment. Ecol Eng. 2008;34(3):207–214.

[14] Renman A, Renman G, Gustafsson JP, Hylander L. Metal removal by bed filter materials used in domestic wastewater treatment. J Hazard Mater. 2009;166(2–3):734–739.

[15] Heistad A, Paruch AM, Vråle L, Adam K, Jenssen PD. A high-performance compact filter system treating domestic wastewater. Ecol Eng. 2006;28(4):374–379.

[16] Joy DM, King R, Maunoir S, Philip H. Field testing of the Eparco Compact Filter wastewater system. Proceedings of the 10th National Symposium on Individual and Small Community Sewage Systems – On-Site Wastewater Treatment. March 21–24; Sacramento, California; 2004. p. 298–308.

[17] Lamichhane KM. On-site sanitation: a viable alternative to modern wastewater treatment plants. Water Sci Technol. 2007;55(1–2):433–440.
[18] Bouchet C. On-site sanitation: a strained market [Assaini ssement non-collectif: Un marché sous tension]. Eau, l'Industrie, les Nuisances. 2013;361:34–48.
[19] Stakman WP, Valk GA, van der Harst GG. Determination of soil moisture retention curves. I Sand box apparatus (range pF 0 to 2.7). Institute for Land and Water Management Research. Wageningen, Pays Bas. 1969. p. 19.
[20] Weaver W, Stecher MC, McInnes KJ. Water flow patterns in subsurface flow constructed wetlands designed for on-site domestic wastewater treatment. Environ Technol. 2003;24(1):77–86.
[21] Williams CF, Nelson SD. Comparison of rhodamine-WT and bromide as a tracer for elucidating internal wetland flow dynamics. Ecol Eng. 2011;37:1492–1498.
[22] Wang Y, Song X, Liao W, et al. Impacts of inlet–outlet configuration, flow rate and filter size on hydraulic behavior of quasi-2-dimensional horizontal constructed wetland: NaCl and dye tracer test. Ecol Eng. 2014;69:177–185.
[23] Persson J, Wittgren HB. How hydrological and hydraulic conditions affect performance of ponds. Ecol Eng. 2003;21:259–269.
[24] Wanko A, Zhang JB, Mose R, Gregoire C, Sadowski A. Hydraulic parameters and statistical residence time distribution moments correlations - a lysimeter study for pesticides mitigation. Int J Environ An Ch. 2010;90:299–310. doi:10.1080/03067310902999140
[25] Lange J, Schuetz T, Gregoire C, et al. Multi-tracer experiments to characterise contaminant mitigation capacities for different types of artificial wetlands. Int J Environ An Ch. 2011;91:768–785.
[26] Levenspiel O. Chemical reaction engineering. 3rd ed. New York: John Wiley & Sons; 1998.
[27] Delmas H, Wilhelm AM. Ecoulements dans les réacteurs: distribution des Temps de Séjour, Cours INP Toulouse ENSIACET, 2007, 22p.
[28] Kadlec RH, Wallace SD. Treatment wetlands. Boca Raton, FL: CRC Press; 2009.
[29] Bergonnier S. Relations entre microstructure et propriétés des matériaux enchevetrés. Thèse de Doctorat de l'Université de Paris VI, 2005.
[30] Celzard A, Zhao W, Pizzi A, Fierro V. Mechanical properties of tanning-based rigid foams undergoing compression. Mat Sci Eng A-Struct. 2010;527(16–17):4438–4446.
[31] Šimůnek J, van Genuchten MTh. Modeling nonequilibrium flow and transport with HYDRUS. Vadose Zone Journal. 2008;7(2):782–797.
[32] Molle P, Liénard A, Boutin C, Merlin G, Iwema A. How to treat raw sewage with constructed wetlands: an overview of the French system. Water Sci Technol. 2005;51(9):11–21.
[33] Molle P, Liénard A, Grasmick A, Iwema A. Effect of reeds and feeding operations on hydraulic behaviour of vertical flow constructed wetlands under hydraulic overloads. Water Res. 2006;40:606–612.
[34] Bodin H, Persson J, Englund JE, Milberg P. Influence of residence time analyses on estimates of wetland hydraulics and pollutant removal. J Hydrol. 2013;501:1–12.